Characterization of the Breakaway Al Content in Alumina-Forming Alloys

B. A. Pint, L. R. Walker and I. G. Wright
Metals and Ceramics Division
Oak Ridge National Laboratory
Oak Ridge, TN 37831-6156

Abstract

Residual Al contents were measured in Fe- and Ni-base alloys in order to improve lifetime prediction models based on the consumption of the Al reservoir. Measurements were made using electron probe microanalysis (EPMA) on both foil (50-125µm thickness) and plate (0.5-2mm) material. For FeCrAl, NiCrAl and Fe_3Al plate specimens, significant Al concentration gradients were measured. An Al gradient is not considered in current reservoir type models. Residual Al contents at the onset of breakaway oxidation were somewhat lower than previously reported for several FeCrAl alloys and significantly higher (≈10at.%) for Fe_3Al and Fe-Al alloys. The implications of these results for performance and lifetime predictions are discussed.

Introduction

The oxidation performance of alumina-forming alloys has been widely studied but recent emphasis has been on modeling their failure in order to better predict their oxidation-limited service lifetime. Initial modeling work on Ni-base alloys and coatings fitted specimen mass change data and calculated times and exposure temperatures to critical mass losses.[1-6] This strategy was applicable to NiAl and Ni-base coatings where much faster degradation occurs when the Ni_3Al phase begins to form due to loss of Al.[2,7] A different strategy has been used for modeling the performance of Fe-base alumina-formers, especially oxide dispersion-strengthened (ODS) FeCrAl, where a lifetime model[8-10], which predicts the time to breakaway oxidation based on the consumption of the available Al reservoir, has been used[11-16]

For any oxidation-resistant alloy, the basic definition of the exposure time to breakaway failure at a given oxidation temperature is the time required for the concentration at the alloy-oxide interface of

the element required to form the protective oxide scale (e.g. Cr or Al) to fall to some critical level (C_{bi}) at which protection breaks down. This critical concentration is different from that calculated from thermodynamic considerations because of the kinetic factors involved in the growth of the oxide scale and interdiffusion in the alloy. Growth of the oxide results in preferential consumption of the element of interest and its depletion from the alloy surface regions. If the rate of removal by oxidation is faster than the rate of diffusion of the element from the bulk of the alloy, then a concentration gradient will develop. Thus for chromia formers, it would be anticipated that at breakaway, the Cr concentration at the metal-scale interface would be C_{bi} while the residual Cr content in the center of the alloy at breakaway would be some higher concentration, C_{br}.

For alloys designed to form alumina scales, such as NiAl, FeCrAl-type alloys and iron aluminides (Fe_3Al), the rate of diffusion of Al in the alloy typically is assumed to be faster than the oxidation rate at high temperatures. With no Al gradient, C_{bi} and C_{br} are a constant C_b and the difference between the starting content (C_o) and C_b, along with the component thickness, defines the available Al reservoir.[8-10] These reservoir-type models assume that all of the Al in the alloy in excess of C_b is available to form a protective oxide; thus it is essential to determine C_b in order to accurately model oxidation behavior. The value of C_b potentially changes depending on the alloy composition,[14,17] microstructure (especially alloy grain size),[18] substrate strength[13] (wrought vs. oxide-dispersed) and exposure temperature.[18]

This study was undertaken to measure C_b values in foil and plate material of various alumina-forming alloys after long-term oxidation exposures, including those which resulted in the breakdown of the alumina scale and the formation of Fe-rich oxide. On plate specimens, 0.5-2mm in thickness, Al gradients were observed in specimens of FeCrAl, Fe_3Al and NiCrAl. The implication of such an observation on performance and modeling failure is discussed using several examples.

Experimental Procedure

The chemical composition of the alloys examined in this study are given in Table I in atom%, which is used throughout this paper. The commercial alloys and foils were provided by the manufacturers, whereas FeCrAl+Y and Fe_3Al+Hf were vacuum induction melted, cast in a water-chilled

Cu mold and annealed 4h at 1300°C. The Allegheny-Ludlum FeCrAl foil (FCAZM) was an experimental laboratory heat containing both Zr and mischmetal (Ce and La) and ODS Fe_3Al was made using a commercial process.[15] Specimen thicknesses varied from 0.4-2mm to foils (40-125μm thickness). In some tests, a wedge-shaped specimen[19] (0.5-2mm variation in thickness) was used. Prior to oxidation, the plate specimens (>0.4mm thickness) were polished to a 0.3μm surface finish on all faces. All specimens were cleaned ultrasonically in acetone and methanol prior to oxidation. Oxidation exposures were conducted in resistively heated furnaces with temperatures of 1050°-1300°C in either laboratory air or dry O_2. Cycle time at temperature was either 1h or 100h (more detailed cyclic exposure experimental procedures are provided elsewhere[20]). Specimen mass gains were measured using a Mettler model AG245 balance. After exposure, the specimens were examined using scanning electron microscopy (SEM) and electron probe microanalysis (EPMA) with a JEOL model 733 or JEOL model 8200. To examine the Al content in the alloy, specimens were Cu-plated, sectioned and metallographically polished. Figure 1 shows an example of the EPMA profiles made on a typical specimen.

Results

Figure 2 gives an example of the measured EPMA profiles in ODS Fe_3Al after 28, 100h cycles at 1300°C, Figure 1a. The locations of the profiles on the metallographically sectioned specimen are indicated in Figure 1a and the EPMA results are summarized in Table II. The profiles shown in Figure 2 indicate that there is not a uniform Al profile in ODS Fe_3Al. Very low levels of Al were measured near the end where breakaway occurred and iron oxide formed. In the first 200μm, the Al level varies considerably which may reflect an internally oxidized zone. Over the next 200μm into the specimen, the Al content increased from 3 to 4.5%. A previous study of the failure of wrought Fe_3Al+Zr measured a residual Al content of 4.8% (2.4wt%) Al and did not detect a gradient over a distance of 20μm into the substrate.[21] At a distance of 1600μm into the ODS Fe_3Al specimen, the Al content was >11%. In the center of the specimen (scan 2), the Al profile did not show a gradient and averaged 12.4%. On the opposite end of the specimen, the Al content increased from 10.3% to over 11%, similar to the content at the opposite end of the specimen at a distance of 1.5mm into the metal. In each scan, the Cr profiles

showed a constant value across the specimen, Figure 2. A second ODS Fe_3Al specimen examined after failure at a much shorter time at 1300°C also showed an Al gradient in one end, but the Al content dropped to only 7.5% at the outer surface of the specimen, Table II. However, this specimen was not sectioned such that the iron oxide region was visible, and it began breakaway oxidation at a much shorter time (1400h) compared to the first specimen (2800h), Table II.

In order to obtain breakaway failures of ODS Fe_3Al at lower temperatures, the cycle time at temperature was reduced from 100h to 1h. An ODS Fe_3Al specimen that failed after 3950, 1h cycles at 1200°C showed Al contents which varied from 7% at the metal-scale interface to 11% near the center of the specimen. This indicates that at 1200°C there were similar Al levels remaining in ODS Fe_3Al as at 1300°C. In both cases, the Al content, >10%, at the center of the specimen was much higher than anticipated and represents a large reservoir of Al that was not consumed and did not contribute to a longer lifetime. The Al content dropped to a much lower level near the breakaway oxidation front but was much higher throughout the rest of the specimen. At the opposite end of the specimen exposed at 1300°C, the Al content beneath a nominally protective scale had dropped to only 10.4% (Scan 3 in Figure 2) suggesting that the critical Al content for ODS Fe_3Al is ≈10%.

Because of the reported differences between ODS and wrought alloys,[13] the Al content of a wrought Fe_3Al+Hf specimen also was measured in order to check for Al gradients. In this case, a 1.5mm thick specimen exposed for 15, 100h cycles was examined, prior to the onset of breakaway oxidation. This specimen showed a very shallow gradient, less than 1% over 5mm, Figure 3, indicating a lack of significant gradient formation during steady state oxidation. The difference between the Al profiles in the wrought and ODS Fe_3Al alloys suggests that the larger Al gradients occur during breakaway oxidation, or that gradients occur only in ODS alloys. Figure 4 shows various measured lifetimes for ODS and Hf-doped Fe_3Al specimens as a function of specimen thickness. Two ODS specimens had lifetimes similar to those observed for Fe_3Al+Hf, one of them being the 1.6mm specimen shown in Figures 1 and 2. However, three other ODS Fe_3Al specimens had substantially shorter lifetimes. It is not clear why such a large scatter was observed, but the presence of an Al gradient in the substrate could account for such variable performance.

Iron aluminide specimens were not the only specimens where Al gradients were observed. Three APM specimens were examined after exposures of 5, 10 and 15, 100h cycles at 1300°C, Table II. Figure 5 compares Al profiles measured at the center and ends of these specimens. In each case, the end of the specimen contained a substantially lower Al content (≤1% Al) than the center of the specimen. However, in two specimens where breakaway oxidation was observed during 100h cycles at 1300°C, no Al gradient was observed in the ends of the specimen to a depth of 1mm (e.g. Figure 5), and fairly uniform values of 0.1% were measured, Table II. A specimen of MA956HT showed a similar residual Al content after failure after 48, 100h cycles at 1200°C, Figure 6a and Table II. A slight gradient existed in the specimen with ≈0%Al detected in the first ≈200µm of material and 0.1-0.2% detected at 400-500µm from the end of the specimen, Figure 6a. For a PM2000 specimen, which failed after 3950, 1h cycles at 1200°C, no gradient was detected to a depth of 6mm from the end of the specimen. A slight gradient was observed for a PM2000 specimen after 31, 100h cycles at 1300°C, Figure 6b. Both a profile at the specimen end and one near the center showed an Al content of 0.1% to a depth of ≈200µm and then a 0.2% content. In each of these ODS FeCrAl specimens, the residual Al content appeared to be significantly lower than the value of 2-2.6% (1-1.3wt.%) in other studies.[8,9,14]

A more extensive experimental study is being performed on the effect of oxidation temperature and specimen thickness (initially using parallelepipeds) on the time to breakaway oxidation for MA956 in order to improve lifetime predictions. Thinner specimens (0.5-0.75mm) have been examined after failures at 1200°, 1250° and 1300°C, Figure 7a and Table II. The 0.75mm thick specimen exposed at 1250°C for 5, 100h cycles showed a significant difference between the center of the specimen and the end where breakaway oxidation occurred. From the end of the specimen, the Al content was ≈0.1% to a depth of 650µm. However, near the center of the specimen, the Al content was 1.1-1.2%. A similar Al content was measured near the center of the 0.75mm thick MA956 specimen exposed at 1300°C for 3, 100h cycles, Figure 7a. However, the 0.5mm thick specimen exposed at 1200°C for 11, 100h cycles showed a much lower Al content at the center, with an average value of 0.2%. A 0.5mm thick MA956 specimen which failed after 350, 1h cycles at 1200°C showed a residual Al content of 0.1% to a depth of 1.5mm into the specimen and an average Al content of 0.2% in cross-section, Table II.

The difference in final Al content among the various specimens may be due to their different thicknesses, but it also may be an effect of oxidation temperature. Figure 8 shows some results for the time to breakaway for MA956 specimens as a function of time at different oxidation temperatures. During 100h cyclic exposures at 1250° and 1300°C, increasing the specimen thickness did not produce a uniform increase in time to breakaway oxidation. A similar response was found for specimens exposed to 1h cycles at 1200°C. Particularly for the thicker specimens in each case, there did not appear to be a significant increase in lifetime compared to thinner specimens. The existence of Al gradients in the thicker specimens may explain the limited benefit of increasing thickness as more Al at the center of a thick specimen is left unconsumed at breakaway. In contrast, for the specimens exposed in 100h cycles at 1200°C, where little gradient was observed after failure, a more uniform increase in time to breakaway with specimen thickness was observed for specimens from 0.5-1.5mm in thickness, Figure 8.

Along with plate specimens, foil specimens also were characterized. In general, the foil specimens of FeCrAl, alloy 214 and PM2000 tended to have little or no gradients, Table II. This is not surprising given the short diffusion distance. For breakaway failures at 1050° and 1100°C, FCAZM had no residual Al content, i.e. C_b=0. Likewise, Haynes 214 foil showed no residual Al content after failure at 1100°C, Table II. The PM2000 foil had average residual Al contents of 0.3% after failure at both 1050°C and 1100°C, which is only slightly higher than values measured at higher temperatures in plate material, Table II. The lower C_b values, combined with less scale spallation, resulted in longer lifetimes for the ingot-processed foils at 1050° and 1100°C, Table II.

Besides PM2000, plate specimens of the other foil compositions also were examined. A 0.7mm thick FeCrAl+Y specimen oxidized to breakaway at 1200°C for 2600, 1h cycles showed no residual Al, similar to the FeCrAl foil, Table II. For comparison to ODS Fe_3Al and PM2000, a 1.5mm thick FeCrAl+Y specimen had a lifetime of 8800, 1h cycles at 1200°C. The much longer life for FeCrAl+Y was attributed to a lower C_b value. Alloy 214 also was examined in plate form at 1100°C and 1200°C. A plate specimen was examined after 10,000h at 1100°C. Figure 9 shows that Al gradients had developed in the specimen both at the end of the specimen and also at the center of the specimen. These gradients may explain the limited effect of specimen thickness on the time to breakaway oxidation at 1200°C,

Figure 10. For this Ni-base alloy in 1h cycles at 1200°C, breakaway was signalled by the onset of very high mass losses rather than a region oxidizing to all oxide, as in Figure 1a. The relatively short lifetimes found at 1200°C for alloy 214 (Figure 10) indicate that this alloy is limited to lower temperature applications, even with thicker cross-sections.

Another example of a type of alloy which undergoes early breakaway failure due to the formation of Al gradients is ferritic Fe-Al, such as Fe-15Al+Hf. This material showed breakaway oxidation after 11, 100h cycles at 1100°C, and Fe-13Al+Hf after an even shorter exposure, Figure 11. The failures were not proceeded by any measured scale spallation. In Fe-15Al+Hf, a steep Al gradient was measured in the end close to the accelerated attack, Figure 12, while a large quantity of Al (only slightly less than the starting Al content of the alloy, Table I) remained near the center of the specimen. The early breakaway was not observed with a higher Al content (Fe-20Al+Hf) or when Cr was added to the alloy (Fe-13Al-5Cr+Hf). The beneficial effect of Cr, which may decrease C_b, is consistent with a "third element" effect.[14,22]

The residual Al content also was evaluated in wedge-shaped specimens of MA956HT and ODS Fe_3Al. In these specimens, an Al gradient is nominally expected since the specimen began with a thickness variation from 0.5mm at the tip to 2mm at the opposite end. In a MA956HT wedge exposed for 28, 100h cycles at 1200°C, the Al content varied from 0% for the first 400μm of remaining metal to ≈7%, 7mm into the specimen, Figure 13. In an ODS Fe_3Al wedge exposed for 12, 100h cycles at 1300°C, the Al content varied from ≈6% Al at the specimen tip, to ≈16% Al 2mm into the specimen, and ≈18% Al 12mm from the tip, Figure 14. This minimum value of Al in the gradient was between the 2 observed in "flat" specimens exposed at 1300°C, Table II.

Figure 15 shows the oxidation performance for the wedge specimens at 1200°C in 100h cycles compared to flat specimens of the same material. For MA956HT, the wedge specimen showed a 40% shorter life (28 cycles) than a 1.0mm thick specimen (48 cycles). With a tip thickness of 0.5mm, the failure time of the wedge specimen was comparable to that expected for a 0.5mm thick flat specimen. However, the ODS Fe_3Al wedge specimen showed breakaway oxidation after 75 cycles while a 0.5mm thick specimen failed after 39 cycles. Despite the Al gradient, the ODS Fe_3Al wedge specimen lasted

considerably longer than expected. Considering that gradients form in flat specimens as well as wedge-shaped specimens, it is not clear what information is gained from examining wedge-shaped specimens.

Discussion

In general, the residual Al contents reported here for ODS FeCrAl are lower than those from several earlier studies and higher for Fe_3Al. Also, the presence of significant Al gradients in Fe_3Al and FeCrAl has not been previously reported. Gradients in NiCrAl had been expected given phase changes (e.g. β depletion) near the oxidation front[23-25] and their limited life in 1200°C exposures.[16] The presence of Al gradients in Fe-base alloys is a significant issue that needs to be considered in order to accurately model time to failure, especially in thicker specimens. The current reservoir-type models do not consider the formation of concentration gradients, and failure is anticipated to occur with a substrate that has a uniform Al content throughout. The application of the concepts of intrinsic chemical failure or mechanically induced failure[26] to alumina-forming alloys needs to be reconsidered. It is possible that both types of failure occur with similarly low values of C_{bi} but scale spallation leads to failures with higher C_{br} values.

Gurrappa et al.[14] showed no Al gradients in ODS FeCrAl variants oxidized at 1100°-1200°C for various times. However, all of those specimens were 0.5mm thick or less, and the composition was only reported at one section. Therefore, while there was no face-to-face gradient in those relatively thin specimens, this does not prove that there are no end-to-end gradients or that gradients might develop in thicker specimens at these temperatures. Aluminum concentration profiles may be flat in the majority of cases but, where such a gradient exists, a reservoir-type model may not be very accurate in predicting time to failure.

The presence of Al concentration gradients is extremely important to the performance of Fe_3Al and Fe-Al materials. Iron aluminides were thought to have strong promise for long lifetimes in high temperature environments because of their large Al reservoir. However, their high coefficient of thermal expansion (CTE) results in more scale spallation compared to FeCrAl-base alloys and thus a faster rate of Al consumption.[15,27] When faster Al consumption is combined with a much higher C_b than previously

thought,[11,12,15,21] the advantage of iron aluminides over FeCrAl is negligible. After correcting for thickness differences of specimens tested in 1h cycles at 1200°C, ODS Fe_3Al has only a slightly longer lifetime than ODS FeCrAl, and Fe_3Al+Hf has only a slight advantage over FeCrAl+Y.[20]

The observation of high residual Al contents at the center of ODS Fe_3Al specimens was not especially surprising. With only ≈2%Cr in the alloy (compared to ≈20%Cr in FeCrAl-type alloys), there is not enough Cr to have a third element effect which may involve increasing the Al activity.[22] Similarly, reducing the Cr content in FeCrAl was found to increase C_b.[14] Implications of the higher residual Al contents in ODS Fe_3Al are significant. The value previously used for C_b was 4.8% (2.4wt.%). However, when Al gradients are taken into account, this measurement[21] likely reflected C_{bi} (as described in the Introduction) rather than a true C_b which implies no Al gradients exist. The values measured in the center of ODS Fe_3Al specimens actually are values of C_{br} but are likely a better reflection of C_b than the interfacial Al content. In the reservoir model, increasing C_b to ≈10% will significantly reduce previous lifetime predictions at 1000°-1200°C.[11,12,15,16] However, the formation of Al gradients in ODS Fe_3Al may explain their erratic performance in 1300°C testing, Figure 4.

Ferritic Fe-Al alloys (≤22%Al) have better spallation resistance than Fe_3Al because of their lower CTE.[28] By staying away from the intermetallic phase, these materials may combine sulfidation and carburization resistance with better alumina scale adhesion than Fe_3Al, and so be useful for coating applications. However, they have a somewhat limited Al reservoir due to their high C_b, and their performance has been difficult to assess because of unexpected early failures, e.g. Figure 11. While Fe-15Al+Hf failed after 1100h at 1100°C, it has not failed after 4000h at 1200°C, suggesting that there may be lower Al concentration gradients at 1200°C. The Al gradient measured after exposure at 1100°C explains the early failure, but it is not clear why such a large gradient developed. With a ferritic structure, it might be expected that the Al diffusivity would be similar to that of FeCrAl. Longer lifetimes at 1100°C were observed for alloys with higher Al contents and by the addition of Cr, Figure 11. However, moving to a finer-grained alloy microstructure could reduce the formation of Al gradients by increasing the effective Al diffusivity in the alloy.[18]

A study of Hf-doped Fe-Al alloys showed that specimens of cast, Fe-9.9%Al+Hf appeared to

have an Al content less than a critical value, since the time to breakaway oxidation at 1000°-1200°C was essentially zero.[29] Thus, 10%Al appears to be a reasonable estimation of C_b for modeling both wrought and ODS Fe-Al base materials. Whenever the Al content drops below ≈10%, whether because of an Al gradient or overall Al consumption, breakaway oxidation is likely to occur.

The development of Al concentration gradients in MA956 may explain some of the observations of lower than expected lifetimes as a function of thickness and temperature, Figure 8. As mentioned above, the thicker specimens of MA956 did not continue to show an essentially linearly-increasing time to breakaway as indicated by thinner specimens. However, this was not observed for specimens exposed for 100h cycles at 1200°C where no Al concentration gradient was observed. Figure 16 compares the experimental data at 1250°C with lifetimes predicted using a reservoir model with different C_b values. Generally, the experimental data match lifetimes predicted with C_b values between 1-2%. Note that the measured residual Al content in the 0.7mm thick specimen varied between 0.1% for C_{bi} and 1.2% for C_{br}. In practice, thinner specimens had longer lifetimes than might have been predicted. This may have been due to reduced Al gradients in the thinner specimens, or because the thinner specimens are weaker and may show improved scale adhesion because of their lower creep strength.[13,30]

Previously, C_b values were calculated based on mass changes of ODS FeCrAl at breakaway.[13] These calculations indicated higher values for C_b in thicker specimens and in ODS FeCrAl compared to wrought or powder metallurgy-based FeCrAl. Higher C_b values for thick ODS FeCrAl specimens were attributed to spallation or mechanically induced failure. In light of the current results, these calculations appear flawed because Al concentration gradients were not considered. Those calculations may reflect some average value of Al remaining in the specimen or an effective C_b; however, the important value for a mechanistic understanding of breakaway oxidation is C_{bi}. Based on the current results, C_{bi} appears to be similar for all FeCrAl alloys and independent of substrate strength and specimen thickness. For example, FeCrAlYshowed a C_{bi} of zero at 1200°C, but so did MA956HT over a distance of 200µm from the end of the specimen, Figure 6a. After breakaway at 1300°C, specimens of APM and PM2000 showed C_{bi} values of 0.1% Al, Figures 5b and 6b. Thus both intrinsic chemical failure at longer times of the more spallation resistant FeCrAlY and spallation induced failure of ODS FeCrAl alloys at shorter times

occurred with similar values of C_{bi}. The largest difference between ODS and wrought FeCrAl was observed for foil material tested at 1050° and 1100°C, Table II. In this case, specimens of PM2000 foil showed higher C_b values without an Al gradient and more scale spallation, which may be attributed to the much higher strength of the PM2000 foil.[31]

The results from MA956 indicated some increase in C_{br} as a function of exposure temperature, Figure 7. For PM2000, little effect of temperature was noted, Table II. However, due to the presence of Al concentration gradients and thickness variations in the specimens examined, further work will be necessary to verify this relationship. A theoretical examination of the transition from internal to external oxidation calculated the parameter N_B, the critical mole fraction of the solute B (in this case, Al) for the transition, which basically compares the square root of the ratio of the parabolic rate constant to the Al diffusivity.[32] A calculation of N_B using FeCrAl kinetic data from this study and others[12,15,20,29] and Al diffusion data from the literature[33] suggests that N_B would increase with temperature, Figure 17, which may be an indication that C_{bi} may also increase with temperature. Since there appear to be many factors involved in determining C_{bi} and C_{br}, it may be that their variation with temperature needs to be evaluated for each class of material.

Aluminum concentration gradients were not observed in all specimens. The foil materials had fairly uniform Al contents at failure, so that current lifetime models should be accurate for foil specimens. Also, ingot-processed FeCrAl had no residual Al content and thus no gradient after testing. The full use of the Al reservoir led to exceptionally long lifetimes for this class of materials in both foil and plate form, Table II. An early study[34] of FeCrAlY performance measured a residual Al content of 1.2% (0.6wt.%) after 3000h at 1200°C in a 0.5-0.8mm thick sheet, and did not report the presence of an Al concentration gradient. Although APM showed Al gradients in specimens stopped prior to the onset of failure at 1300°C, two failed specimens showed little gradient immediately after failure, Figure 5. Also, essentially no gradient was measured for specimens of MA956HT and PM2000, which showed similar oxidation performance.

Obviously the formation of an Al concentration gradient is determined by the relative rates of diffusion in the alloy and consumption by oxidation which vary with temperature and time. Examining

the results of a wide range of materials and exposure conditions has helped in identify factors that are important to the formation of an Al concentration gradient:

(1) Specimen geometry. The specimen ends and especially corners on parallelepiped specimens are regions of high surface area/volume. A higher rate of consumption in these areas will likely result in variations in Al content across the specimen.

(2) Scale adhesion. This is especially relevant for iron aluminides because of their relatively high CTE and ODS alloys which are known to exhibit more scale spallation than less creep-resistant wrought alloys.[20,30] With increased scale spallation, a higher Al consumption rate is expected which may lead to Al gradients.

(3) Alloy grain size. As mentioned above, finer grained alloys allow faster Al transport and have been shown to produce lower values of C_b in Fe-Al alloys.[18] Coarse-grained alloys may be more prone to producing Al concentration gradients. However, these grain size observations are all from Fe-Al alloys and may not be relevant to FeCrAl-type alloys, although all are ferritic.

(4) Low Cr content. Empirically, alloys such as Fe-Al and Fe_3Al have high C_b levels and tend to exhibit Al depletion gradients, but the reasons are not clear. Higher Cr levels may increase Al diffusivity, thus reducing gradients. Also, these alloys may be more susceptible to spallation assisted failures rather than intrinsic chemical failure,[26] which could affect the Al profile when breakaway occurs.

One additional issue that has not been considered is that many of the specimens contain different types of reactive element additions, Table I. Aside from oxide dispersions vs. alloy additions, it is not known if these different RE additions affect C_{bi}. Until there is a better understanding of all of the relevant factors, it will be difficult to develop improved lifetime models.

Summary

The residual Al content was measured in ferritic FeCrAl and Fe-Al, Fe_3Al as well as NiCrAl specimens exposed for various times and temperatures and with varying specimen thicknesses. Values were reported which differed from earlier studies. Higher values were measured for Fe-Al and Fe_3Al and somewhat lower values were measured for FeCrAl. Surprisingly, in each class of material, examples

were found where the Al concentration profile was not flat and significant gradients existed in the specimen. Thus, in some cases rather than measuring a uniform Al concentration (C_b), the Al concentration at the metal-scale interface (C_{bi}) was significantly different than the Al concentration at the center of the specimen (C_{br}). For Fe-Al and Fe_3Al, C_{bi} varied from 2.5-7.7%Al and C_{br} from 10-12%. However, in most FeCrAl specimens, the gradient was minimal by the time the specimen reached breakaway oxidation. Comparing values of C_{bi} in various FeCrAl alloys, there was little effect of substrate strength on its value at 1200°-1300°C. In many cases, the presence or absence of gradients could be explained by the diffusion length, i.e. specimen thickness or geometry. The presence of Al concentration gradients could have a significant effect on the oxidation-limited lifetime realized in service and needs to be considered in lifetime models.

Acknowledgments

The authors would like to thank G. Garner, L. D. Chitwood, J. W. Jones and H. Longmire at ORNL and summer students C. Simpson, N. Bonwit, C. Roberts and J. Schenning for assistance with the experimental work, and D. F. Wilson and P. F. Tortorelli at ORNL for their comments on the manuscript. The alloys were provided by M. Harper, Special Metals (MA956, MA956HT), D. Spörer, Plansee (PM2000), B. Jönsson, Kanthal (APM), M. Harper, Haynes (214) and R. Klug, Allegheny-Ludlum (FCAZM). This research was sponsored by the U.S. Department of Energy, Fossil Energy Advanced Research Materials Program under contract DE-AC05-00OR22725 with UT-Battelle, LLC.

References

1. Lowell, C. E., Smialek, J. L. and Barrett, C. A., Cyclic oxidation of superalloys. In: *High-Temperature Corrosion*, (Ed. R. A. Rapp) NACE, Houston, TX, pp.219-226 (1983).
2. Doychak, J., Barrett, C. A., and Smialek, J. L., Oxidation between 1000°C and 1600°C and limiting criteria for the use of Zr-doped β-NiAl and β/γ' alloys. In: *Corrosion & Particle Erosion at High Temperature* (Eds. V. Srinivasan and K. Vedula), TMS, Warrendale, PA, pp.487-514 (1989).
3. Lowell, C. E., Barrett, C. A., Palmer, R. W., Auping, J. V. and Probst, H. B., COSP: A computer

model of cyclic oxidation. *Oxid. Met.*, **36**, 81-112 (1991).

4. Nesbitt, J. A., Vinarcik, E. J., Barrett, C. A. and Doychak, J., Diffusional transport and predicting oxidative failure during cyclic oxidation of β-NiAl alloys. *Mater. Sci. Eng.*, **A153**, 561-6 (1992).
5. Nesbitt, J. A. and Lowell, C. E., Prediction of the high temperature oxidative life of intermetallics. In: *High Temperature Ordered Intermetallics V*, Symp. Proc. v.288, I. Baker, R. Darolia, J. D. Whittenberger and M. H. Yoo, Eds. (MRS, Pittsburgh, PA, 1993) p.107-18.
6. Smialek, J. L., Nesbitt, J. A., Barrett, C. A. and Lowell, C. E., Cyclic oxidation testing and modelling: A NASA Lewis perspective. In: *Cyclic Oxidation of High Temperature Materials* (Eds. M. Schütze and W. J. Quadakkers) Institute of Materials, London, UK, pp.148-68 (1999).
7. Smialek, J. L. and Lowell, C. E., Effects of diffusion on aluminum depletion and degradation of NiAl coatings. *J. Electrochem. Soc.*, **121**, 800-5 (1974).
8. Quadakkers, W. J. and Bennett, M. J., Oxidation induced lifetime limits of thin walled, iron based, alumina forming, oxide dispersion strengthened alloy components. *Mater. Sci. Tech.*, **10**, 126-31 (1994).
9. Quadakkers, W. J. and Bongartz, K., The prediction of breakaway oxidation for alumina forming ODS alloys using oxidation diagrams. *Werkst. Korros.*, **45**, 232-41 (1994).
10. Quadakkers, W. J., Bongartz, K. and Schubert, F., The prediction of oxidation limited life of thin walled ODS heat exchangers for high temperature applications. In: *Materials for Advanced Power Engineering II* (Eds. D. Coutsouradis, et al.) Kluwer Academic Publishers, Dordrecht, Netherlands, pp.1533-42 (1994).
11. Wright, I. G., Pint, B. A., Simpson, C. S. and Tortorelli, P. F., High temperature oxidation life characteristics of ODS Fe_3Al. *Mater. Sci. Forum*, **251-254**, 195-202 (1997).
12. Pint, B. A., Tortorelli, P. F. and Wright, I .G., Long-term oxidation performance of ingot-produced Fe_3Al alloys. *Mater. High Temp.*, **16**, 1-13 (1999).
13. Wilber, J. P., Bennett, M. J. and Nicholls, J. R., Life-time extension of alumina forming FeCrAl-RE alloys: Influence of alloy thickness. *Mater. High Temp.*, **17**, 125-32 (2000).
14. Gurrappa, I., Weinbruch, S., Naumenko, D. and Quadakkers, W. J., Factors governing breakaway oxidation of FeCrAl-based alloys. *Mater. Corr.*, **51**, 224-35 (2000).
15. Wright, I. G., Pint, B. A. and Tortorelli, P. F., The high temperature oxidation behavior of ODS Fe_3Al. *Oxid. Met.*, **55**, 333-57 (2001).
16. Wright, I. G., Pint, B. A., Hall, L. M. and Tortorelli, P. F. Experimental results and modeling related to oxidation lifetimes. In: *Lifetime Modelling of High Temperature Corrosion Processes*. (Eds. M. Schütze, W. J. Quadakkers and J. R. Nicholls) Maney, London, pp.339-58 (2001).
17. Quadakkers, W. J., Clemens, D. and Bennett, M. J., Measures to improve the oxidation limited service life of Fe-Based ODS alloys. In: *Microscopy of Oxidation 3* (Eds. S. B. Newcomb and J. A. Little), Institute of Metals, London, U.K., pp.195-206 (1997).
18. Pint, B. A., Leibowitz, J. and DeVan, J. H., The effect of an oxide dispersion on the critical Al content in Fe-Al Alloys. *Oxid. Met.*, **51** (1999) 183-99.

19. Tatlock, G. and Al-Badairy, H., The application of a wedge-shaped sample technique for the study of breakaway oxidation in Fe-20%Cr-5Al base alloys. *Oxid. Met.*, **53** (2000) 157-70.
20. Pint, B. A., Tortorelli, P. F., and Wright, I. G., Effect of cycle frequency on high temperature oxidation behavior of alumina-forming alloys. *Oxid. Met.*, **58**, 73-101 (2002).
21. Bennett, M. J., DeVan, J. H. and Tortorelli, P. F., The oxidation behaviour of iron aluminides at 1300°C. In: *Microscopy of Oxidation 3* (Eds. S. B. Newcomb and J. A. Little) Institute of Metals, London, U.K., pp.233-45 (1997).
22. Stott, F. H., Wood, G. C. and Stringer, J., The influence of alloying elements on the development and maintenance of protective scales. *Oxid. Met.*, **44**, 113-45 (1995).
23. Nesbitt, J. A. and Heckel, R. W., Diffusional transport during the cyclic oxidation of $\gamma + \beta$, Ni-Cr-Al (Y, Zr) alloys. *Oxid. Met.*, **29**, 75-102 (1988).
24. Clemens, D., Vosberg, V., Penkalla, H. J., Breuer, U., Quadakkers, W. J. and Nickel, H., TEM and SNMS studies on the oxidation behaviour of NiCrAlY-based coatings. *Fresenius J. Anal Chem.*, *358*, 122-6 (1997).
25. Pint, B. A., More, K. L., Wright, I. G. and Tortorelli, P. F., Characterization of thermally cycled alumina scales. *Mater. High Temp.*, **17**, 165-71 (2000).
26. Evans, H. E., Donaldson, A. T. and Gilmour, T. C., Mechanisms of breakaway oxidation and application to a chromia-forming steel. *Oxid. Met.*, **52**, 379-402 (1999).
27. Pint, B. A., More, K. L., Tortorelli, P. F., Porter, W. D. and Wright, I. G., Optimizing the imperfect oxidation performance of iron aluminides. *Mater. Sci. Forum*, **369-372**, 411-8 (2001).
28. Pint, B. A., Zhang, Y., Tortorelli, P. F., Haynes, J. A. and Wright, I. G., Evaluation of iron-aluminide CVD coatings for high temperature corrosion protection. *Mater. High Temp.*, **18**, 185-92 (2001).
29. Pint, B. A., Unpublished research, Oak Ridge National Laboratory, Oak Ridge, TN, 2002.
30. Evans, H. E., Nicholls, J. R. and Saunders, S. R. J., The influence of diffusion-related mechanisms in limiting oxide-scale failure. *Solid State Phenom.*, **41**, 137-56 (1995).
31. Pint, B. A., Swindeman, R. W., More, K. L. and Tortorelli, P. F., Materials selection for high temperature (750°-1000°C) metallic recuperators for improved efficiency microturbines. ASME Paper #2001-GT-445, presented at the International Gas Turbine & Aeroengine Congress & Exhibition, New Orleans, LA, June 4-7, 2001.
32. Wagner, C., *Z. Elektrochem.*, **63**, 772 (1959).
33. Heeseman, A., Schmidtke, E., Faupel, F., Kolb-Telieps, A. and Klower, J., Al and Si diffusion in FeCrAl alloys. *Scripta Mater.*, **40**, 517-522 (1999).
34. Antill, J. E. and Peakall, K. A., Influence of an alloy addition of Y on the oxidation behaviour of an austenitic and a ferritic stainless steel in carbon dioxide. *J. Iron Steel Inst.*, **205**, 1136-4 (1967).

List of Figures

Figure 1. (a) Light microscopy of polished cross-section of ODS Fe_3Al oxidized for 28x100h at 1300°C. A thick non-uniform oxide covers the specimen except at the left end where breakaway oxidation has begun oxidizing the entire section. Three EPMAline scans are indicated. (b) schematic showing standard scans.

Figure 2. EPMAAl and Cr line scans from the ODS Fe_3Al specimen in Figure 1a. Near the iron oxide, a different profile was detected. The Cr content was uniform in all three areas.

Figure 3. EPMA Al and Cr line scans from 1.49mm thick Fe_3Al+Hf specimen oxidized for 15, 100h cycles at 1300°C. Very little Al gradient was observed in this specimen.

Figure 4. Time to breakaway as a function of specimen thickness for several materials in 100h cycles at 1300°C. The behavior of ODS Fe_3Al was less predictable than the other materials.

Figure 5. EPMAAl line scans from 3 different APM specimens oxidized for different times at 1300°C. In the two thicker specimens examined before breakaway oxidation had occurred, there was a substantial difference in the Al content in the end of the specimen compared to the center of the specimen.

Figure 6. EPMAAl line scan from (a) the end of a MA956HT specimen oxidized for 48, 100h cycles at 1200°C and (b) a PM2000 specimen oxidized for 31, 100h cycles at 1300°C. Neither show a significant Al gradient.

Figure 7. EPMA Al line scans from several different MA956 specimens (a) oxidized to breakaway at 1200°C-1300°C and (b) oxidized to shorter times at 1200°C.

Figure 8. Time to breakaway as a function of specimen thickness for MA956 in 4 different cyclic tests.

Figure 9. EPMAAl and Cr line scans from alloy 214 oxidized for 100, 100h cycles at 1100°C. A slight Al gradient was observed in both the end of the specimen and near the center of the specimen.

Figure 10. Time to breakaway as a function of specimen thickness for alloy 214 and MA956 during 1h cycles at 1200°C in dry O_2. Even thick 214 specimens failed in relatively short times in this test.

Figure 11. Total (specimen + spalled oxide) mass gain for several Hf-doped Fe-Al alloys during 100h cycles at 1100°C in laboratory air. Breakaway failures were observed for some specimens.

Figure 12. EPMAAl line scans from Fe-15Al+Hf oxidized for 17, 100h cycles at 1100°C. A strong Al gradient was observed near the end of the specimen which went into breakaway.

Figure 13. EPMAAl line scans from the MA956HT wedge specimen oxidized for 2800h at 1200°C.

Figure 14. EPMAAl line scans from the ODS Fe_3Al wedge specimen oxidized for 1200h at 1300°C.

Figure 15. Total and specimen mass gains for plate and wedge specimens of MA956HT and ODS Fe_3Al oxidized in 100h cycles at 1200°C.

Figure 16. Time to breakaway as a function of specimen thickness for MA956 oxidized in 100h cycles at 1250°C. The experimental data points are plotted along with predicted lifetimes with different C_b levels.

Figure 17. Values of N_B as a function of temperature calculated using parabolic rate constants from cyclicly and isothermally exposed FeCrAl specimens.

Table I. Chemical composition (in atomic%) of alloys examined in this study obtained by inductively coupled plasma analysis and combustion analysis.

Alloys:	MA956	MA956HT	PM2000	APM	FeCrAl	FeCrAl	ODS Fe_3Al	Fe_3Al+Hf	Fe-Al+Hf	Alloy 214
Dopant(s):	Y_2O_3	Y_2O_3	Y_2O_3	ZrO_2	Zr,Ce,La	Y	Y_2O_3	Hf	Hf	Y,Zr
Fe	69.45	65.78	69.40	68.09	68.79	69.83	69.35	70.15	84.79	3.37
Ni	0.07	0.04	0.09		0.20	<0.01	0.02	<0.01	<0.01	70.54
Cr	20.07	21.74	18.91	20.37	20.21	20.21	2.13	1.96	0.01	16.73
Al	8.78	10.68	9.82	10.65	10.24	9.86	27.07	27.67	15.09	8.73
Si	0.13	0.11	0.07	0.43	0.15	<0.01	0.05	<0.01	0.02	0.16
Ti	0.40	0.43	0.49	0.03	0.005	<0.01	<0.01	<0.01	<0.01	0.01
Y	0.24	0.23	0.22	<0.01		0.082	0.21	<0.003	<0.01	0.0025
Zr	<0.01	<0.01	<0.01	0.057	0.036	<0.01	<0.01	<0.01	<0.01	0.0120
Other	0.01 Cu	0.01 Cu	0.01 Cu	0.08 Mn	0.003 **Ce**	0.01 Cu	0.01 Cu	0.10 **Hf**	0.052 **Hf**	0.17 Mn
	0.03 Co	0.02 Co	0.01 Co		0.002 **La**			0.01 Cu		0.02 Co
	0.01 W	0.02 Mo	0.01 W		0.22 Mn					0.01 Mo
	0.08 Mn	0.06 Mn			0.009 Mg					
	0.02 V	0.03 V			0.016 V					
B	<0.005	<0.005	<0.005			<0.005	<0.005	0.013	0.014	0.005
P	0.014	0.008	<0.01		0.030	<0.01	0.012	0.006	0.007	0.007
C	0.064	0.170	0.043	0.130	0.078	<0.04	0.158	0.080	0.004	0.225
N (ppma)	608	1065	104		140	11	3480	<4	15	101
O (ppma)	6490	6779	8050	1710		110	6160	120	139	48
S (ppma)	41	71	34	16	5	16	30	36	45	5

Table II. Average residual Al contents for various specimens oxidized to failure at time t_b or shorter times.

Alloy	Thickness	Temperature	t_b(h)	Cycle Frequency	C_0(at.%)	Residual Al (at.%)
ORNL ODS Fe_3Al	1.6mm	1300°C	2800	100h		2.5-12.4
	1.7mm	1300°C	1400	100h		7.5-10.5
	1.5mm	1200°C	3950	1h	27.1	7.0-11
Fe_3Al+Hf	1.5mm	1300°C	1500*	100h	27.7	17.5-18.3
Fe-15Al+Hf	1.5mm	1100°C	1100	100h	15.1	7.7-14.8
APM (FeCrAl + Zr)	1.4mm	1300°C	500*	100h	10.7	3.0-5.9
	1.7mm	1300°C	1000*	100h		2.6-3.5
	1.8mm	1300°C	1500*	100h		0.4-1.4
	1.3mm	1300°C	1500	100h		0.1
	1.9mm	1300°C	1700	100h		0.1
MA956HT (ODS FeCrAl)	1mm	1200°C	4800	100h	11.0	0.1
MA956 (ODS FeCrAl)	0.5mm	1200°C	350	1h	8.4	0.1-0.2
	0.5mm	1200°C	1100	100h		0.2
	1.5mm	1200°C	1000*	100h		7.0-7.2
	0.75mm	1250°C	500	100h		0.3-1.2
	0.75mm	1300°C	300	100h		1.2
PM2000 (ODS FeCrAl)	40 µm	1050°C	350	1h	9.8	0.3
	40 µm	1100°C	125	1h		0.3
	1.7mm	1200°C	3950	1h		0.2
	1.6mm	1300°C	3100	100h		0.2
FeCrAl+Zr/Ce/La	60 µm	1050°C	2100	1h	10.2	0
	60 µm	1100°C	750	1h		0
FeCrAl + Y	0.7mm	1200°C	2600	1h	9.9	0
Alloy 214	60 µm	1100°C	400	1h	8.7	0
	1.4mm	1100°C	10000*	100h		7.0-8.3

*specimen removed from test prior to breakaway oxidation

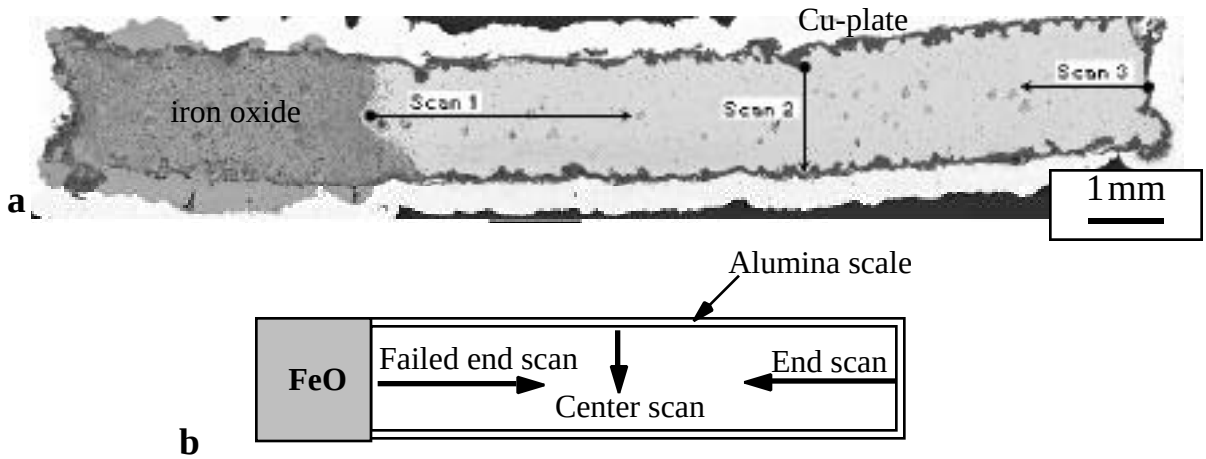

Figure 1. (a) Light microscopy of polished cross-section of ODS Fe_3Al oxidized for 28x100h at 1300°C. A thick non-uniform oxide covers the specimen except at the left end where breakaway oxidation has begun oxidizing the entire section. Three EPMAline scans are indicated. (b) schematic showing standard scans.

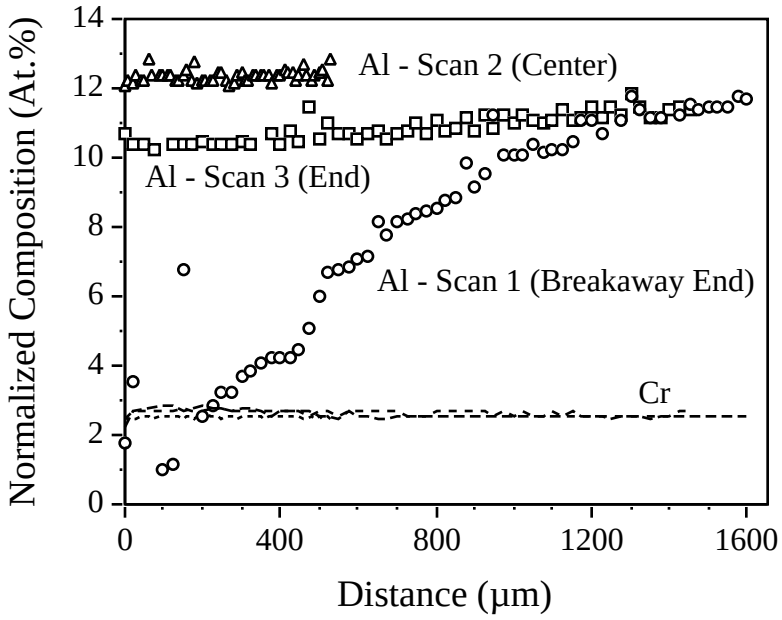

Figure 2. EPMAAl and Cr line scans from the ODS Fe_3Al specimen in Figure 1a. Near the iron oxide, a different profile was detected. The Cr content was uniform in all three areas.

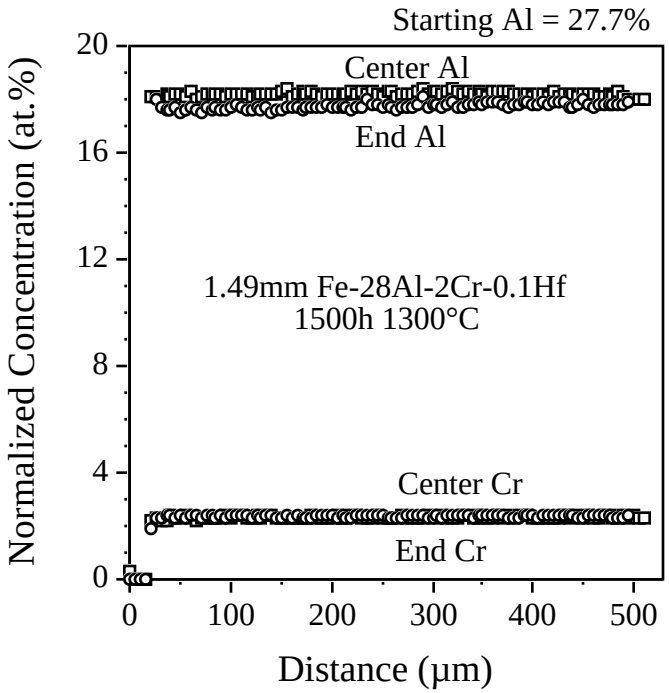

Figure 3. EPMA Al and Cr line scans from 1.49mm thick Fe_3Al+Hf specimen oxidized for 15, 100h cycles at 1300°C. Very little Al gradient was observed in this specimen.

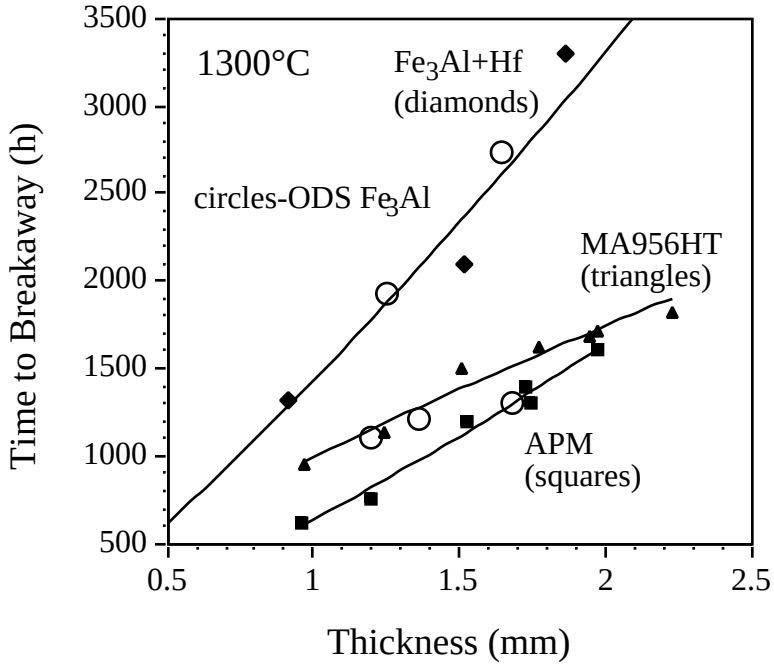

Figure 4. Time to breakaway as a function of specimen thickness for several materials in 100h cycles at 1300°C. The behavior of ODS Fe_3Al was less predictable than the other materials.

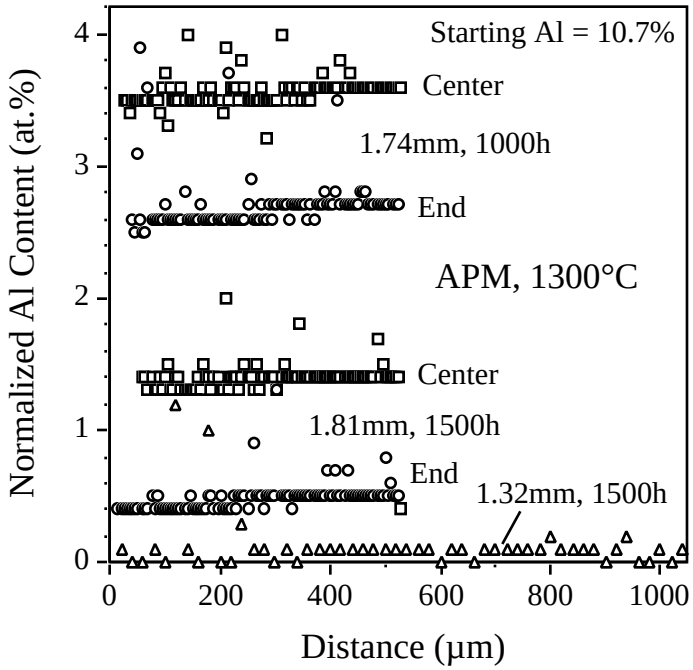

Figure 5. EPMAAl line scans from 3 different APM specimens oxidized for different times at 1300°C. In the two thicker specimens examined before breakaway oxidation had occurred, there was a substantial difference in the Al content in the end of the specimen compared to the center of the specimen.

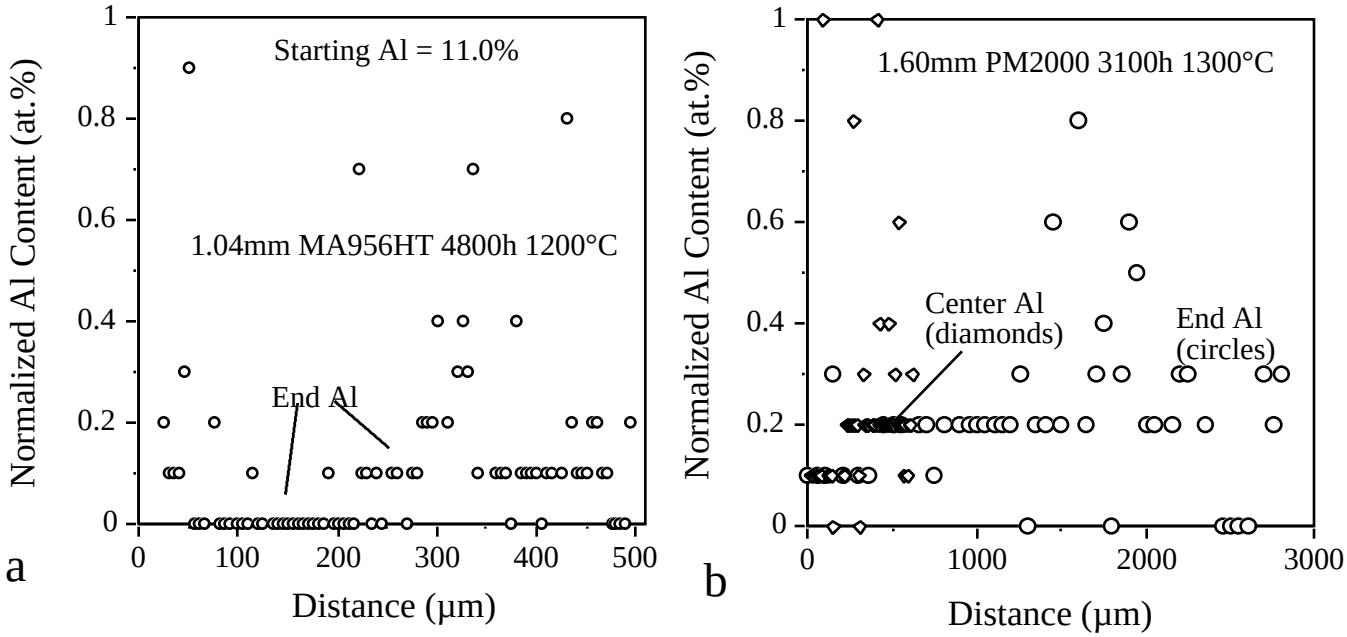

Figure 6. EPMAAl line scan from (a) the end of a MA956HT specimen oxidized for 48, 100h cycles at 1200°C and (b) a PM2000 specimen oxidized for 31, 100h cycles at 1300°C. Neither show a significant Al gradient.

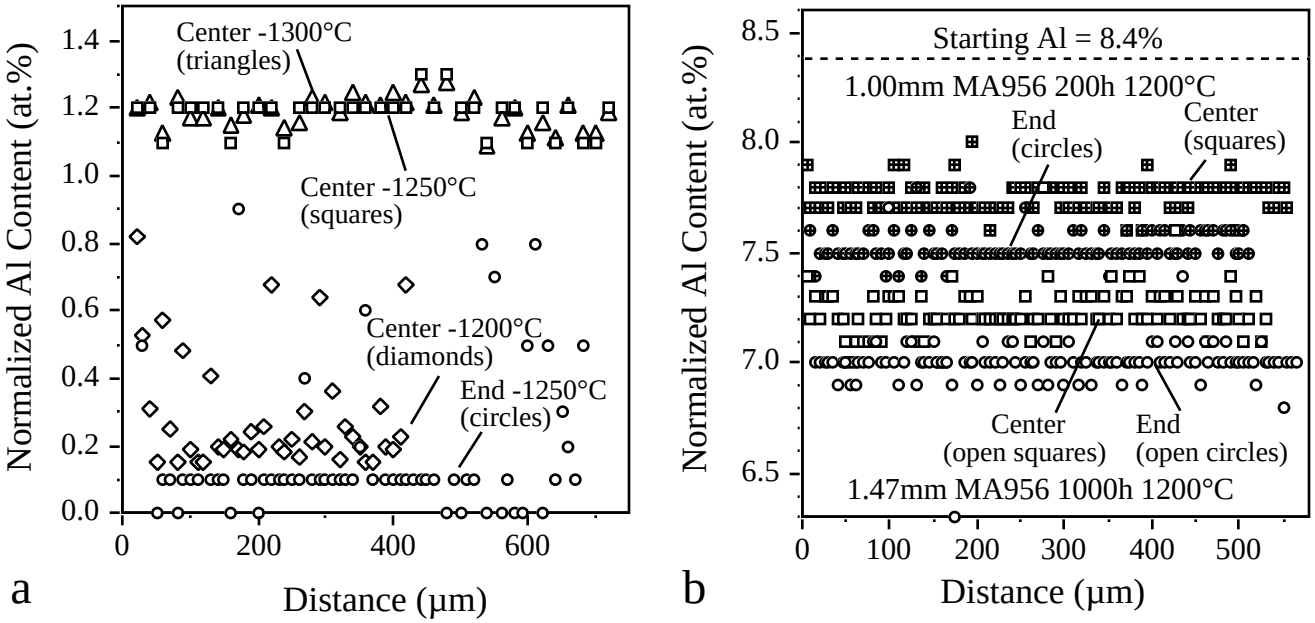

Figure 7. EPMA Al line scans from several different MA956 specimens (a) oxidized to breakaway at 1200°C-1300°C and (b) oxidized to shorter times at 1200°C.

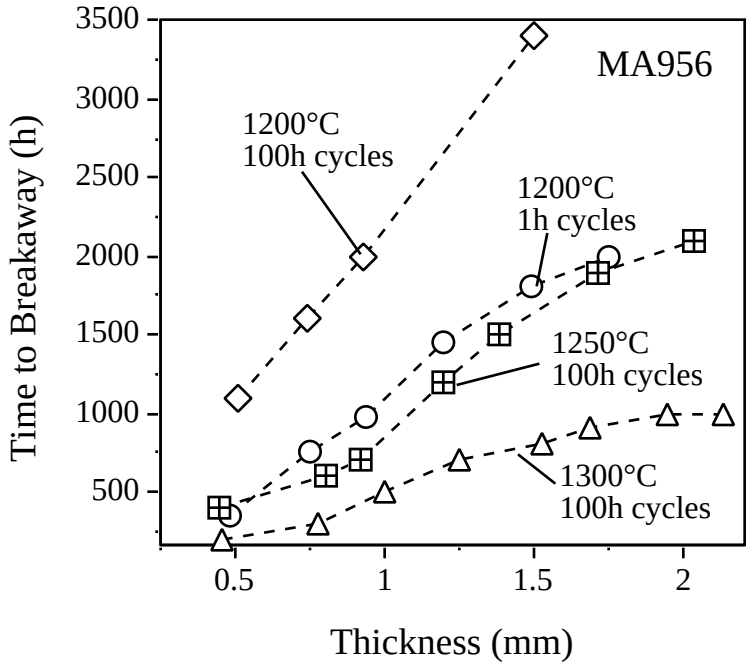

Figure 8. Time to breakaway as a function of specimen thickness for MA956 in 4 different cyclic tests.

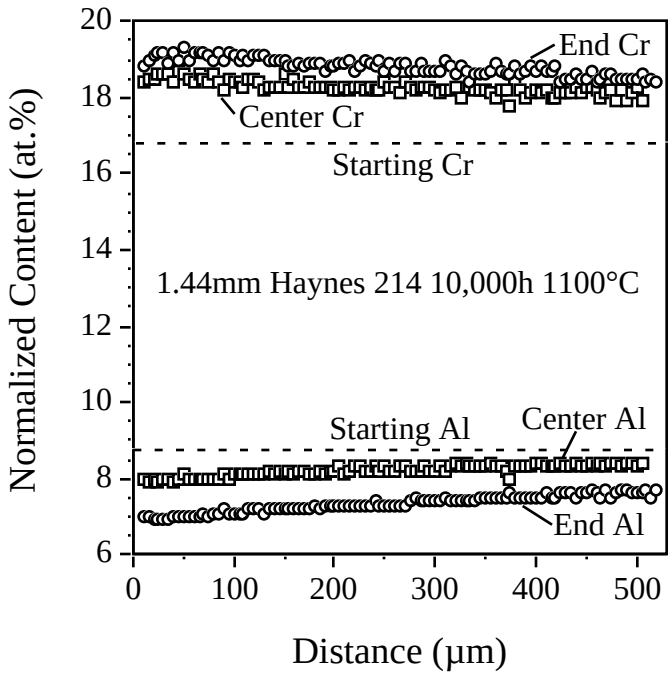

Figure 9. EPMAAl and Cr line scans from alloy 214 oxidized for 100, 100h cycles at 1100°C. A slight Al gradient was observed in both the end of the specimen and near the center of the specimen.

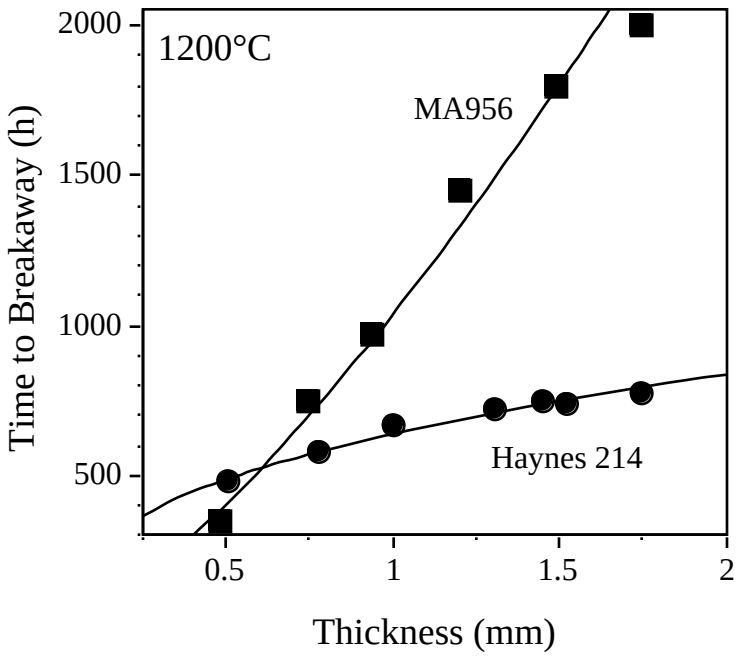

Figure 10. Time to breakaway as a function of specimen thickness for alloy 214 and MA956 during 1h cycles at 1200°C in dry O_2. Even thick 214 specimens failed in relatively short times in this test.

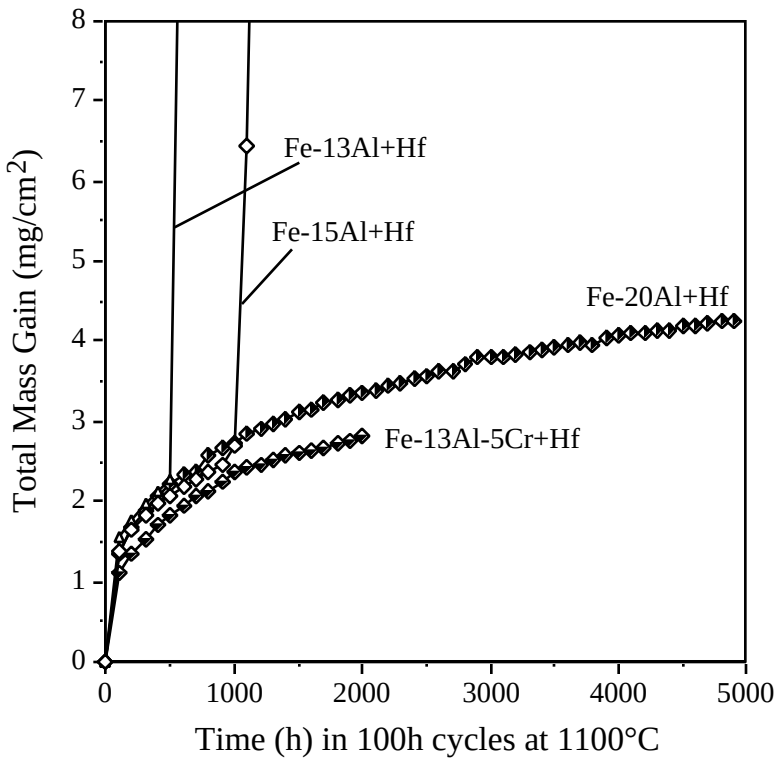

Figure 11. Total (specimen + spalled oxide) mass gain for several Hf-doped Fe-Al alloys during 100h cycles at 1100°C in laboratory air. Breakaway failures were observed for some specimens.

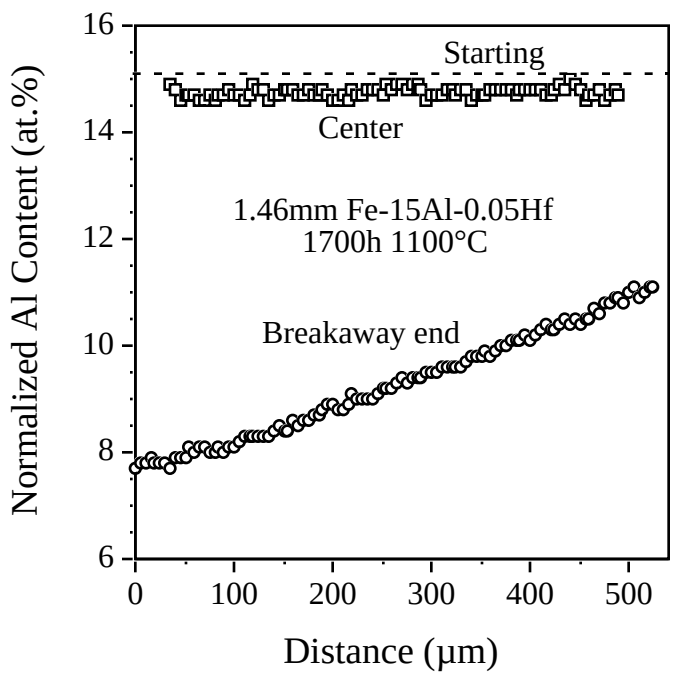

Figure 12. EPMAAl line scans from Fe-15Al+Hf oxidized for 17, 100h cycles at 1100°C. A strong Al gradient was observed near the end of the specimen which went into breakaway.

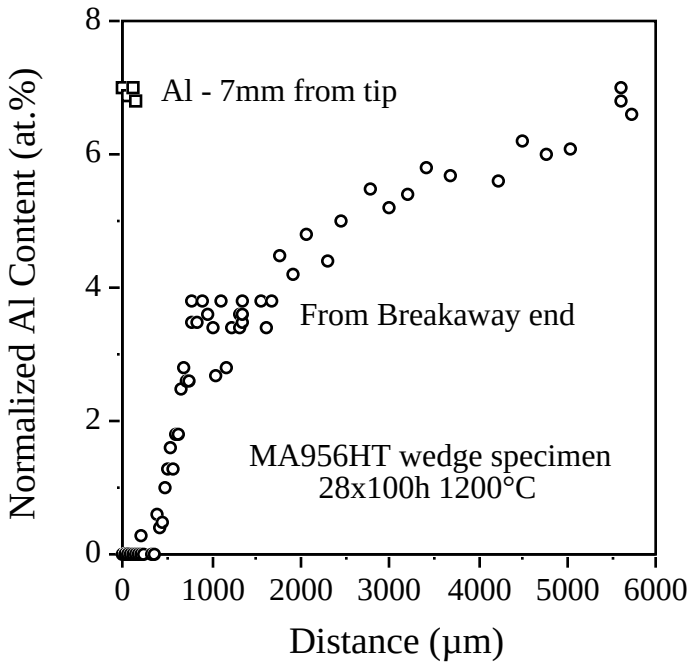

Figure 13. EPMAAl line scans from the MA956HT wedge specimen oxidized for 2800h at 1200°C.

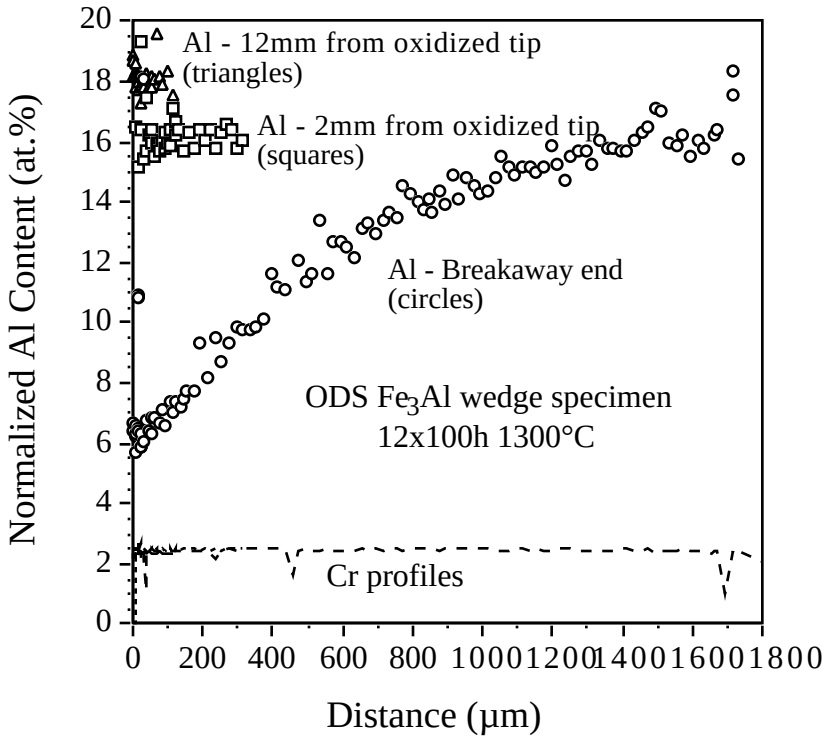

Figure 14. EPMAAl line scans from the ODS Fe_3Al wedge specimen oxidized for 1200h at 1300°C.

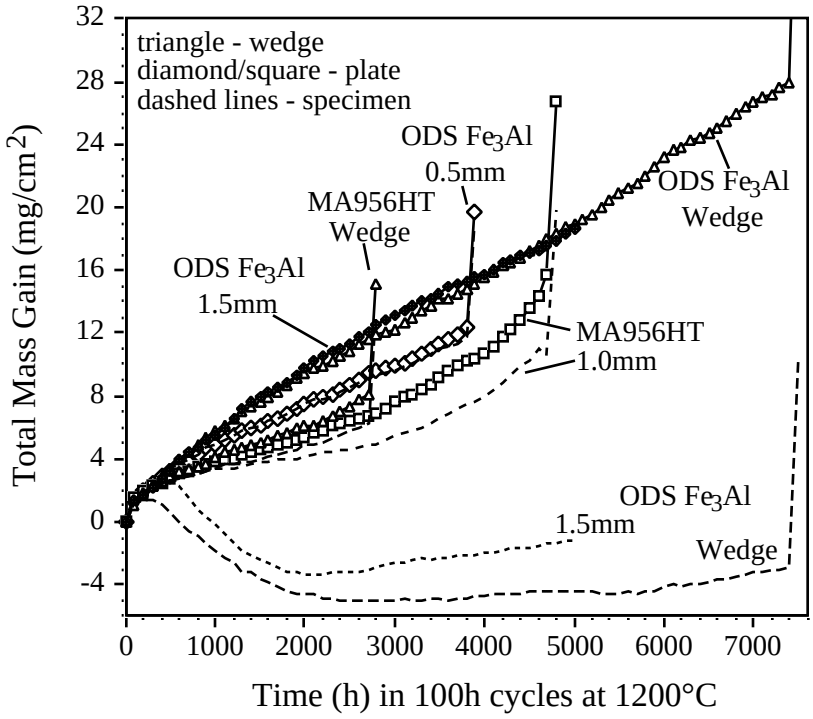

Figure 15. Total and specimen mass gains for plate and wedge specimens of MA956HT and ODS Fe_3Al oxidized in 100h cycles at 1200°C.

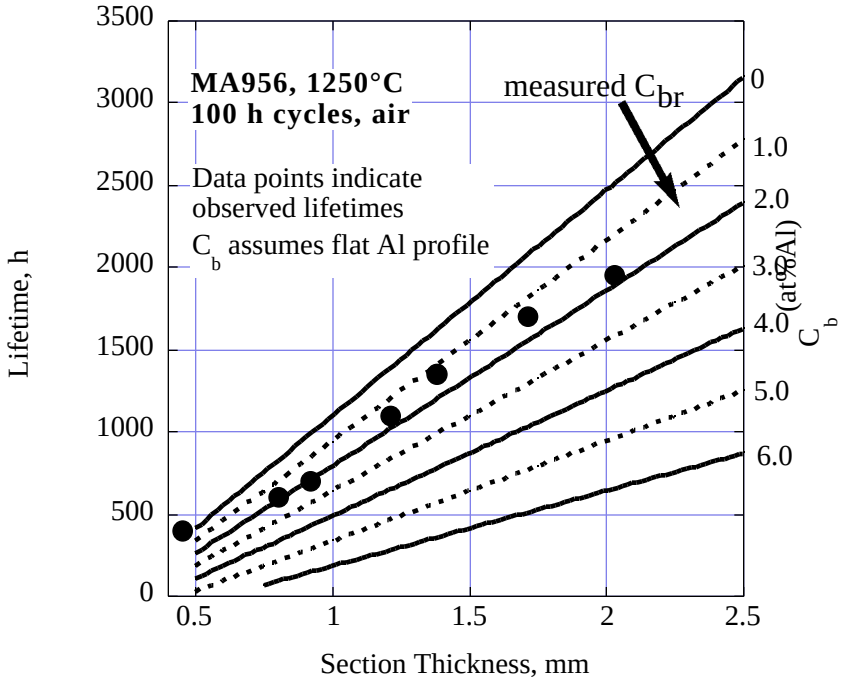

Figure 16. Time to breakaway as a function of specimen thickness for MA956 oxidized in 100h cycles at 1250°C. The experimental data points are plotted along with predicted lifetimes with different C_b levels.

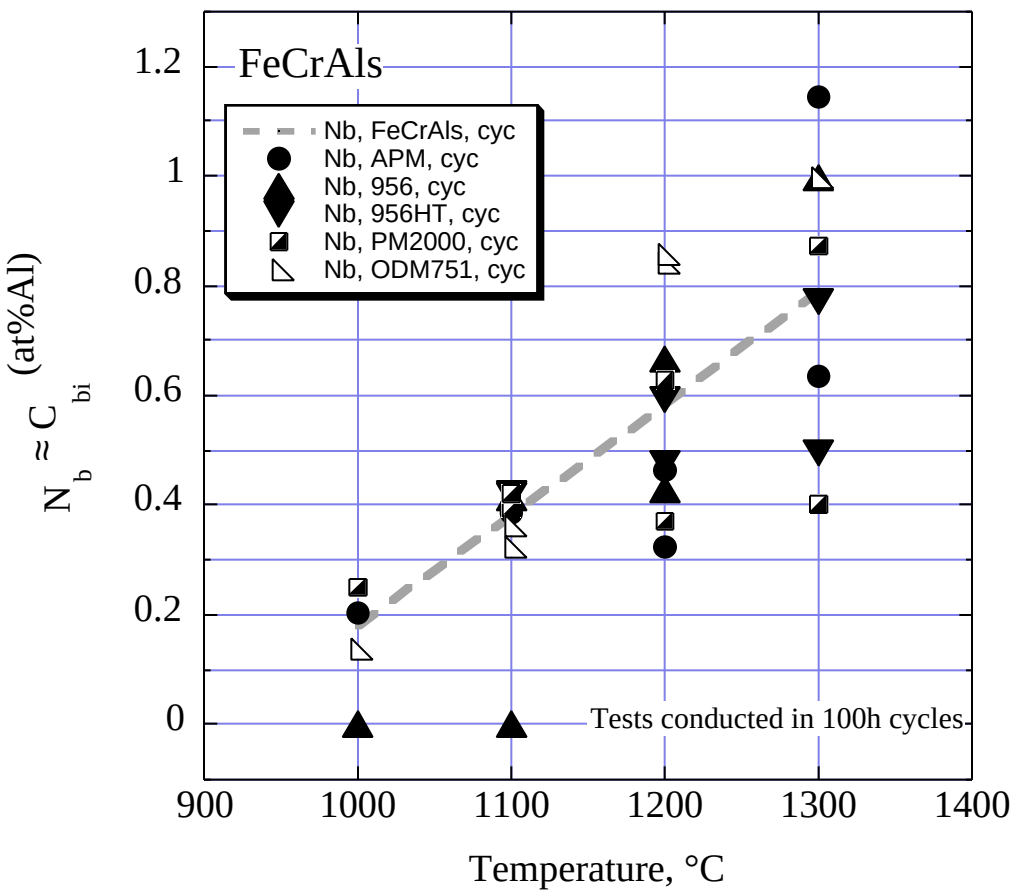

Figure 17. Values of N_B as a function of temperature calculated using parabolic rate constants from cyclicly and isothermally exposed FeCrAl specimens.